Egyptian Journal of Chemistry

http://ejchem.journals.ekb.eg/

Application of Low-Cost Adsorption Technique on Organic Pollutant Dye Removal by Bio-Waste Adsorbents

Heba M. El Refay [1], Asmaa M. Raslan [2] and A. M. E. Atia [1]

[1] *Department of Chemistry, Faculty of Science (Gils), Al-Azhar University (Girls), Yousef Abbas Str, P.O. Box:11754, Nasr City, Cairo, Egypt*

[2] *Ministry of Environment, Egptian Environmental Affair Agency, 30 Misr Helwan El-Zyrae Road, Maadi, Cairo, Egypt*

Abstract

This study focused on studying the kinetics, thermodynamics, and the adsorption equilibrium of Acid fuchsin, C.I acid violet 19 (AV19) dye from aqueous media by using different adsorbent such as Caw Animal Bone (CAB) and Hen Eggshell (HES) as a new cheap, low-cost, widely available, eco-friendly, high-efficiency adsorbents. Scanning electron microscopy (SEM) and Fourier transform infrared spectrometer (FTIR) techniques were used to characterize the adsorbent before and after adsorption process. The influence of different conditions had been examined such as pH solution, initial dye concentrations, adsorbent dose, adsorbent sizes, contact time and different temperatures. The equilibrium data was analyzed by Langmuir and Freundlich's isotherm models and showed a good fit with the Langmuir model more than Freundlich's isotherm model (R^2= 0.997), and a pseudo-second order kinetic is the best model suggested to explain the kinetics model with a good agreement with the intra-particle diffusion model. The parameters of thermodynamic including enthalpy ΔH°, entropy ΔS° and free energy ΔG° demonstrated that the adsorption process was feasible, spontaneous, and endothermic in nature of the adsorption of AV19 on CAB and exothermic nature of adsorption of AV19 on HES. The results clarified that a large percentage removal and the optimized conditions were (4±0.2 and 2±0.2) solution pH, 3.82mg/L initial dye concentration, adsorbent dose 0.75 gm/40 ml of particle size (2.36 and 0.355), for CAB and HES respectively and 60 min adsorption time 81.2% and 91.4% of dye was removed by CAB and HES respectively at experimental optimum conditions. The experimental results show that CAB and HES have a good potential as adsorbent to remove the colour from textile effluent and as an alternate low-cost adsorbent.

Keywords: Cow Animal Bone, Hen Egg Shell, Low-Cost Adsorption, Acid violet 19, Adsorption Isotherm, Kinetics.

1. Introduction

Water is an important reason that keeps life and energy on the earth, while millions of people in all the world are facing problems of the lack of fresh and clean drinking water. Industrial progress was the greatest reason of many environmental problems. Large amount of pollutants are rejected into water such as phenol with its derivatives and metal ions. Water pollution and its negative effect on environmental health become the greatest challenges for scientists. The existence of the organic matter in pharmaceuticals, cosmetics, plastics, food, and some other industries produce a large bulk of wastewater yearly **[**1**].** Some of the organic dyes that present in wastewater may decay forming aromatic amines which are cancer-causing under anaerobic conditions, which will be harmful to animals and human. [2].

Nowadays there are over nine million tons of dyes are developed yearly. So, it is of a big challenge to produce a modern technique to manage the problem of wastewater with dyes. Many efforts have been created to produce adsorbents that could destroy dyes from drinking water [3]. treatment of wastewater is very important nowadays because of the required rules for the reduction of different pollutants in water [4].

Artificial dyes are used in many fields of the modern technology, e.g., in a lot of textile industry branches, the tanning of leather industry, in the paper tanning industry, in food processing technology, in the research of agricultural fields, in light-harvesting

*Corresponding author e-mail: hebaelrefay.5919@azhar.edu.eg, (Heba Mohamed El-Refay)

Receive Date: 09 April 2022, **Revise Date:** 25 April 2022, **Accept Date:** 08 May 2022, **First Publish Date:** 08 May 2022

DOI: 10.21608/EJCHEM.2022.132441.5847

arrays, in electro photochemical cells, and hair dying tools. In addition, synthetic dyes were applied to advance the control on wastewater and sewage treatment efficiency also determining the specific surface area of activated mud for the tracing of groundwater, etc. [5].

The dye degradation became so urgent to protect the ecosystem and human health. The using of these aromatic artificial dyes increases daily in different industries mainly in the fabric industries, nowadays the water pollution is the reason of dangerous problems to human and animals [6]. It is of a great interest to concentrate on the dye's adsorption behaviour from water because the low biodegradability, toxicological profile and stability of them. Performance of water decolourization processes can vary significantly along with the adsorbent, dye chemical structure, and operating conditions. sure, the Physio-chemical dye properties have a considerable role in the molecular interactions that observed in the aqueous phase adsorption [7]. Several methods like membrane filtration, advanced chemical oxidation methods, biosorption, adsorption, coagulation/ flocculation, photocatalysis and Ozon treatment method, are applied to eliminate these pollutants. Biosorption method is a suitable technique because of its economic and clean. [7,8].

Adsorption is an active technique in a lot of industrial and natural systems such as separation and purification processes, recovery of chemical compounds, waste treatment processes and biological studies. It can replace with other separation processes and contribute to the removal of contaminants from an aqueous solution [9]. The technique of adsorption is a physicochemical wastewater degradation process that the molecules which dissolved are linked to the adsorbent surface by physicochemical bonds, leading to the development of an adsorbate molecule from the bulk solution to the adsorption place. In last years, it was observed the using of cheap adsorbents for dye decaying, in this study, we focused on generating techniques to clean the wastewater from the organic artificial dyes by an effective and cheap adsorbent [10]. The bones of animals are as an efficient cheap and available adsorbent. There is a considerable capacity of the adsorption of the surface functional groups of the bone regarding the polarizable molecules after suitable modification. great attention paid for the adsorbents that have been modified for the elimination of different organic pollutants like immobilization of proteins or enzymes and organic dyes. These modern applications are because of the functional groups of the adsorbent's surface, which can be modified appropriately [11]. Eggs are one of the most important Food incomes in the framework of world-wide feeding, they are important as a source of vital nutrients to human food such as Proteins, fat-soluble vitamins (A, D, E and K) and trace-minerals like iron and zinc [12]. The shell of the hen egg formed from ceramic molecules that have three-layered structure, called cuticle on the outer shell surface, a spongy or (calcareous) layer and an inner mammillary layer [13].

The mammillary and calcareous layers generate a protein matrix linked to calcite (calcium carbonate) crystal. Also, these layers are well arranged in such a way that contains large number of holes. This arrangement permits the gas exchange through the shell. The outer surface is covered with Mucin protein that considered as a soluble plug for the holes in the shell, also the cuticle is permeable. The percentage (by weight) of the by-product eggshell's chemical components was $MgCO_3$ (1%), $Ca_3(PO_4)_2$ (1%), Organic Material (4%) and $CaCO_3$ (94%) [13]. The eggshell by-product is about 11% of the egg's whole weight (60g) [16]. It was also stated that about 28% of all eggs produced were directed to commercial breaking operations for the egg products formation. [14].

The aim of this research is to use CAB and HES waste by-product as adsorbents adsorbent to removal of AV19 pollutant dye from aqueous media. The effect of variables such as dose of adsorbent, initial dye concentrations, solution pH, contact time, and temperature on dye removal efficiency from aqueous solution was investigated. The adsorption and removal mechanism of CAB and HES on the AV19 were discussed by fitting the isothermal adsorption equation and kinetic equation, the pseudo-first order and pseudo-second-order models were used to investigate the adsorption kinetics. Langmuir and Freundlich isotherm models were used to analyses the equilibrium data. The adsorption's thermodynamic characteristics were also studied, which may provide a new idea for wastewater treatment from toxic azo dye by CAB and HES as adsorbents.

The application of the adsorption method to the process of removing polluting organic ions from wastewater, rather than the most common separation process in current research, by CAB and HES as low-cost, widely available, eco-friendly is novel in this study, and the removal process is characterized by ease of implementation, like the adsorption process.

2. Materials and Methods

2.1. Preparation of adsorbents

In this study, Animal Bone (AB) and Egg Shell (ES) were used as adsorbents for the removal of anionic acid violet 19 dye (AV19). AB were collected from Cow Animal Bone (CAB) and ES collected from Hen Eggshells (HES). HES were collected, then undergo washing process with distilled water and we let them to dry in the oven. After drying, we grounded it and sieved to 150-1000 μm particle size. It was then dried at 105 °C for 24 hours to remove moisture and stored in a closed bottle for later use in adsorption studies [14,15].

CAB were bought from butcher shops and cleaned from any involved meat and fat. Then the undergo washing process for sometimes by water and stayed under air for several days to remove smells, then we had put them in an oven that were adjusted at temperature 80°C to complete the drying process. Then we applied crushing and milling processes on them to produce particles of size range of (3.2, 2.36, and 0.85 mm) then we calcined them for 2 hours at temperature 800°C. The deposit was cleaned using water then dried all night at 100°C in an oven, then calcined at a rate of heating 2°C/min to 400°C and reserved at this temperature for 4h until obtaining a continuing weight. The product was mentioned as the calcined bones (CB) as shown in Photo (1,2) [16].

Photo. 1: HES after preparation

Photo. 2: CAB after preparation

2.2. Preparation of dye solution (adsorbate)

Acid fuchsin dye (Acid violet 19) (AV19) was obtained from El- Gomhoria Company, Egypt and was used without further purification. AV19 was utilized in Andrade's indicator and in various complex stains to demonstrate collagen fibers and in smooth muscle in contrast to collagen. Its molecular formula is $C_{20}H_{17}N_3Na_2O_9S_3$ (mol. wt. 585.5g/L) is chosen as adsorbate Figure (1). The de ionized water was used for preparation of dye stock solution. Dye solution stock of a concentration 1000mg/l was prepared by adding 1 gram of (AV19) in 1 litre distilled water. The experimental solution was prepared by diluting definite volume of the stock solution to get the desired concentration. For absorbance measurements a UV-VIS Spectrophotometer, JAPAN APEL (PD-303S) was employed using quartz cells of path length 1 cm. The maximum wavelength was measured at 543nm.

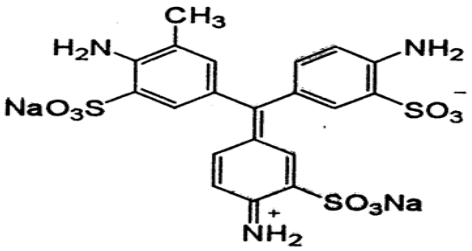

Fig. 1: Chemical Structure of AV19.

2.3. Batch Experimental Setup

Firstly, five various concentrations solutions of AV19 were prepared as Figure (3). Each one of them was then analyzed during a UV-9200 UV- Spectrophotometer. A plot of absorbance versus for every concentration was obtained and λ_{max} of 543nm AV19 was experimentally obtained as show in Figure (2). By applying Beer-Lambert law [14]. ε is that the molar extinction coefficient (O.D. $mole^{-1}$ cm^{-1}) was found to be 0.618 x 10^4 $mole^{-1}$ cm^{-1} for AV19 and R^2 is 0.9993. The study of the effect of several parameters on (AV19) removal by CAB and HES were studied. 40 ml of a certain pH and initial concentration of the dye solutions were taken in 100 ml conical flask, then an appropriate amount of the adsorbent of CAB and HES was added to 40 them, the dye solutions adsorption was carried out at 25±1◦C for a whole day in batch system then a constant speed of shaking (200 rpm) for 30 min was applied, then we applied a separation technique (centrifugation at a rotation speed of 6000 r/min for 5 min) to separate the suspension from the adsorbent, the solution was analyzed after separation for AV19 concentration. The amount of dye adsorbed per unit mass of the adsorbent was analyzed by UV visible spectrophotometer and calculated by Removal % = $(\frac{C_o - C_e}{C_0})$ x 100 [16]. Where C_o is the initial concentration (mg/ L) and C_e is the dye concentration (mg/L) at any time, pH effect on the rate of adsorption was examined and pH values were adjusted with 0.5N HCl and 0.5N NaOH solutions.

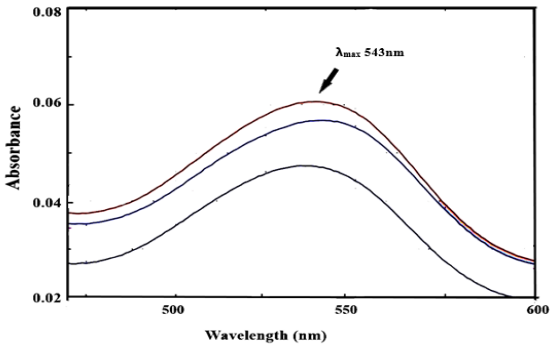

Fig. 2: Absorbance Spectrum of C.I. AV19 dye in visible wavelength

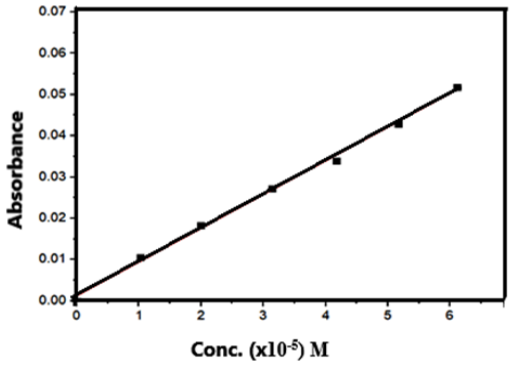

Fig. 3: The molar extinction coefficient of AV19.

3. Results and Discussion

3.1. Surface Characterization

3.1.1. FT-IR spectrum analysis

FT-IR spectrum of CAB as show in Figure 4(a) shows the characteristic bands of hydroxyl apatite (547.84, 625.73 and 988.80) cm^{-1} (shoulder), 1176.15 (shoulder) cm^{-1} due to phosphate vibrations and collagen (C,O) stretching vibration at 1650 cm^{-1}, N–H in plane bending at 1459 cm^{-1}, C–H and N–H stretching modes in (2962.35–3459) cm^{-1} region) [17,18]. Additionally, the standard bands of carbonate substituting for phosphate site (type B) within the apatite lattice also are observed: band at 746.28 cm^{-1} and double bands at 1287.20 /1459 cm^{-1} [19]. The diffractor-gram of CAB presents the hydroxyl apatite pattern. These results prove that the amorphous component was released after calcinations as found within the literature [20]. After AV19 adsorption Figure 4(b), there's a noticeable shift in positions and new peaks appear and a few peaks disappeared. The analysis of the FT-IR spectrum of HES Figure 4(c) discovered the carbonate group presence and proved by the characteristic-peak at 1523 also at 659.39, and 1795.96 cm^{-1}. Furthermore, the observed peaks happen within the area between 3400–3500 and 2516 cm^{-1}, which may be associated with amino-groups. The bands between 2875 and 2982 cm^{-1} characterize carbon bonded hydrogen vibration, signifying the presence of organic layers, formed from amino acids that are involved within the HES, an equivalent opinion was stated by [21]. It had been obvious that after the biosorption of dye Figure 4(d) all the previous mentioned peaks indistinguishably change their positions and therefore the greatest change noticed at the peaks of the carbonate group.

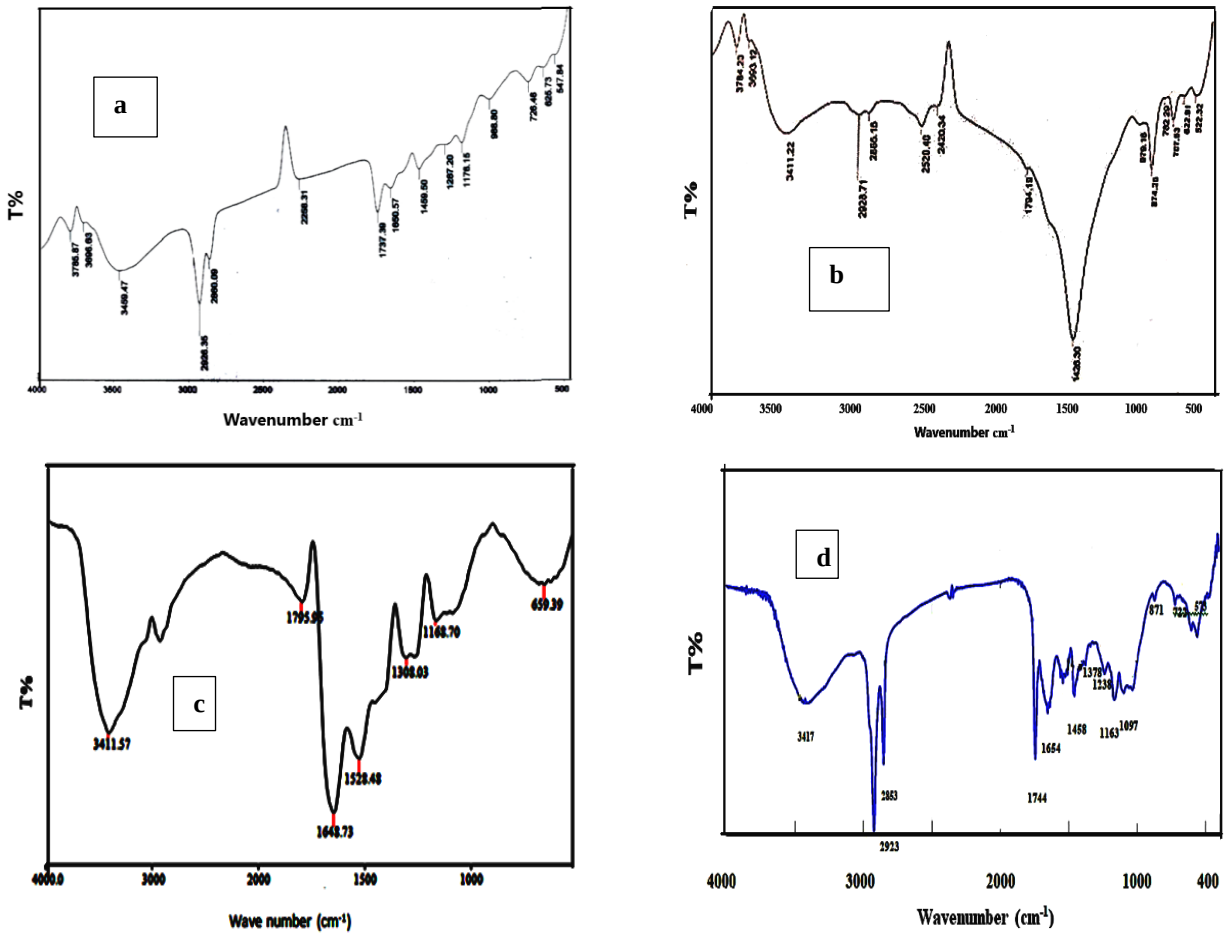

Fig.4: FT-IR Spectrum of (a, c) for CAB and HES before adsorption and (b,d) CAB and HES after AV19 adsorbed.

3.1.2 Scanning Electron (SEM) Analysis

The technique of scanning microscope (SEM) may be a primary device for studying the changes of surface morphology, distribution, and fundamental physical properties of the adsorbents after adsorption. The SEM [analysis] presented in Figure 5(a) shows that the CAB has an accumulation of fine particles of irregular form and size with a quite small ravines [22]. Figure 5(b) Images after AV19 adsorption on CAB shows that more particles are present on the animal surface which becomes rough contains protuberances and thin cylindrical shapes. These particles of AV19. The charged dye molecules are going to be electrostatically interested in the adsorbent's CAB and HES. [23]. Figure 5(c) indicates an irregular pore canal for HES adsorbent particles, columns, and crescent shaped mammillary layers. We noticed that the surface after adsorption Figure 5(d) shows clear pro tubes because of a decent chance for dyes to be trapped and adsorbed into these pores [24].

3.2. Effect of pH Solution

The pH values of the solution are a vital parameter during the adsorption processes. The AV19 adsorption on CAB 45.8 and increase to 81.5 at pH4 while HES surface was 91.5% at pH2 and at 60 min this result show in Figure 7(a and b). The zero-charge point (pH_{pzc}) is a crucial parameter for bio-sorbent to characterize the sensitivity to pH and their surface charges [25]. The pH_{pzc} of the adsorbent was estimated by the solid addition method. The batch equilibrium technique was applied to calculate variables like zero charge point, the effect of pH, and surface chemistry. The activation of acidic or basic functional groups of adsorbents approaches zero at the zero- charge point [26]. The pHpzc was found to be 8, 8.1 for (HES and CAB) samples, respectively meaning that the surface was charged Figure 6(a and b). This result demonstrates that at a pH below 8, the surface of the adsorbents shows positive charges, while at a pH above 8, the surface of the CAB and HES have a negative charge**. S**urface pH of adsorbent is closer to neutral pH. As a result, CAB and HES can be used to adsorb both cationic and anionic moieties**.** The effects of different initial solution pH values on the adsorption of AV19 onto CAB and HES are shown in Figure 7 (a,b) and show that the adsorption of AV19 on HES increases as the solution's pH decreases while the adsorption of AV19 on CAB increase with increase solution's pH and then decrease. The charge on the adsorbent surface may be affected by the initial pH, altering its adsorption capacity. At low pH (< pHpzc, i.e. < 8) the adsorbent surface became highly protonated and was suitable for adsorption of anionic dye causing increased removal percentage of dye this agreement with literature [25]. Also, at high pH (> pHpzc, i.e. > 8) the surface of adsorbent more negative charge so suitable for adsorption of cationic dye. The optimum pH solution for AV19 dye is (4 and 2) for CAB and HES respectively.

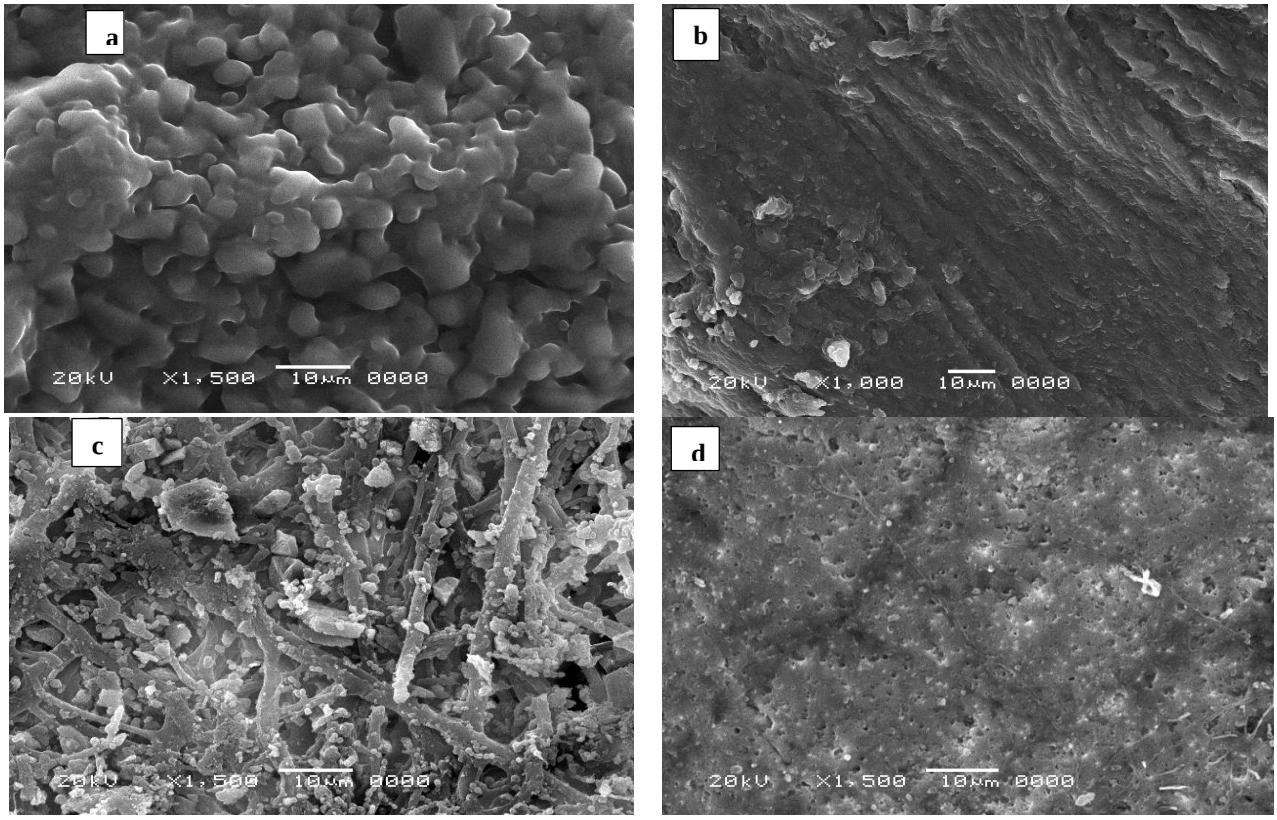

Fig.5: SEM of (a, c) for CAB and HES before adsorption and (b,d) CAB and HES after AV19 adsorbed.

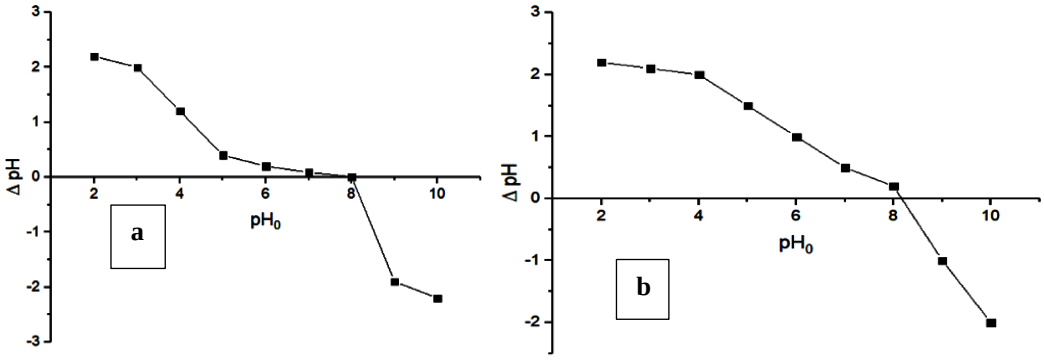

Fig. 6: The Point Zero Charge of (a) HES and (b) CAB.

3.3. Effect of initial dye concentration

The initial adsorbate concentration in solution and therefore the time of equilibrium is an important parameter for the dye up taking from solution by adsorption. Time consumed to approach equilibrium is a very important factor to expect the effectiveness and viability of an adsorbent when it's used to control the pollution [27]. The observed results demonstrate the adsorption capacity is concentration-dependent and reduce with increasing the concentration of the dye. The dye concentration affected the dye diffusion from the solution to the adsorbent's surface. the rise in the dye concentration resulted in a rise in the driving force to the gradient concentration, which helps earlier the diffusion of the dye from the solution into the adsorbent [28]. By increasing dye concentration from (3.81 to 26.74 mg/L) for AV19 The removal percent of AV19 by (CAB and HES) decreased from 83% to 69 you take care of (CAB) and from 86.2 % to 74.5% for (HES), as show in Figure 7(c, d). This phenomenon is attributed to the fact that the available sites for adsorption are higher at lower adsorbate concentrations. However, when the concentration is increased, the available sites become fewer this result agreement with [27].

3.4. Effect of adsorbent dose

A proper quantity of adsorbent is very important for the degradation of concentration of dye from solution and it determined the capacity of adsorbent for the given concentration of adsorbate. It is clear from these results that the rise in the dose amount of the adsorbents led to an increase in the removal degree of AV19 because of the increasing of the number of the available sites for the adsorption of dye [29]. The surface area and therefore the number of empty adsorption sites increase by increasing the adsorbents dose, and this results in increasing the amount of adsorbed dye. After equilibrium, a decrease in the amount of adsorbed particles was noticed. This may attribute to the aggregation or overlapping of the adsorption sites resulting in a decreasing in available adsorbent surface area for dyes and increasing in the length of the path of diffusion [30]. The experiment carried by taking different doses (0.25–1.25g) to seek out the effect of various doses of CAB and HES on the removal of AV19 as show in Figure 7(e, f). The efficiency of removal of AV19 by (CAB and HES) increased from 65.13% to 85.5% and from 64.2% to 85.7%, respectively, when the dose increases from (0.25-0.75g) then decrease to 84% after dose 1.25g for CAB and HES respectively. It had been found that the area increased by increasing the dose of the adsorbent which led to a high dye removal, [31].

3.5. Effect of adsorbent size

The contact surface between the sorbent and therefore the liquid phase could be a great factor that affects the adsorption processes. The particle size effect of CAB and HES on AV19 removal was studied using three particle sizes (3.2 mm, 2.36 mm and 0.85mm) for CAB and (0.85mm, 0.355mm and 0.180 mm) for HES. From Figure 7(g, h) results show that the removal efficiency of AV19 on (CAB and HES) increased from 82% to 88.3% and from 81.2 % to 91.4% when the adsorbent particle size was decrease from (3.2 mm to 0.85mm) for CAB and from (0.850 mm to 0.180mm) for HES after 60 min, respectively. This attributed to by decrease particle size the surface area and active site of both adsorbents increase which suitable for removal of high dye from solution, and this results agreement with literature [22].

3.6. Effect of temperature

A parameter with great significance within the process of sorption is the temperature. A study of the dependence of the temperature on adsorption reactions gives valuable knowledge about the enthalpy and entropy changes during adsorption [32]. From results it has been indicated that the AV19 adsorption on CAB increases with increasing the temperature, but adsorption of AV19 on HES decrease with increasing the temperature. Figure 7(i, j) illustrated that the removal efficiency of AV19 using CAB increase from 82.3% to 88.7% while for HES decrease from 82.6 % to 56.2%. The adsorption capacity of HES decreases by increasing the temperature of the range studied, revealing that the adsorption of AV19 on the HES is exothermic in

nature, and the low temperature promotes adsorption. This effect could be caused by dye molecules being released from the bio sorbent into the aqueous solution as the temperature rises. This result agreement with [29].

3.7. Effect of Contact Time

The kinetic behaviours of the process of adsorption are studied for AV19 under different pH values, concentrations, dose sizes and temperatures. The adsorption process was rapid within the initial 60 min indicating a high affinity between dyes molecules and adsorbents (CAB and HES) surface because of the intra particle diffusion of dye molecules [33,34]. Following this phase, the adsorption process slows suggesting a gradual equilibrium, possibly finally, the saturation is reached, showing the ultimate equilibrium at approximately (60–120 min) for dye, beyond which no further adsorption takes place as show in Figure (7) for CAB and HES. Rapid adsorption of dye in the first 20 min, the adsorption rate slowly increases to reach equilibrium in about 60 min for AV19 on both adsorbents. This can be explained by the fact that the adsorption sites were vacant and easily accessible at the beginning so dye molecules could easily interact with these sites, but after 60 min, the removal of dye got constancy due to equilibrium establishment A similar result has also been reported [33].

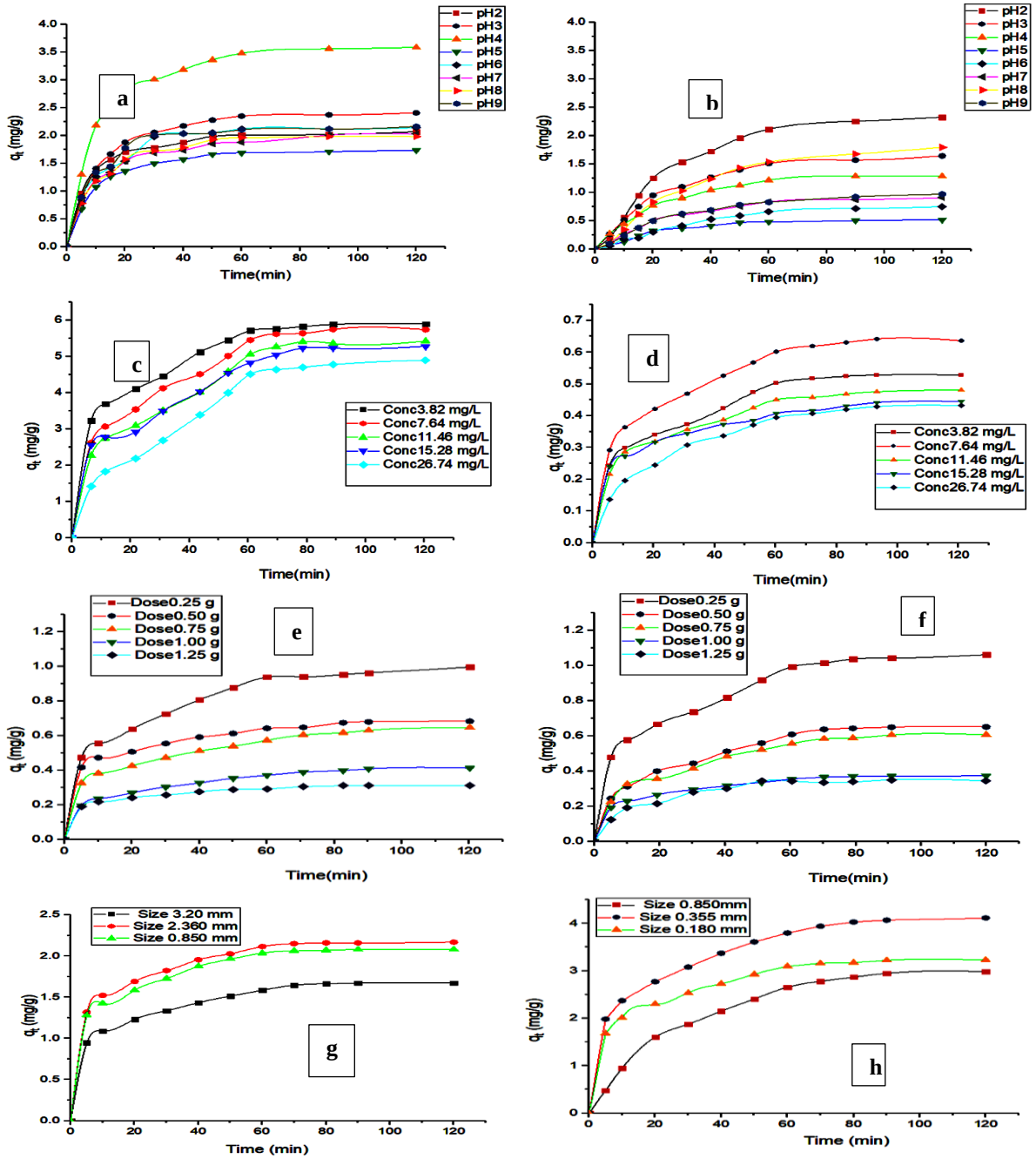

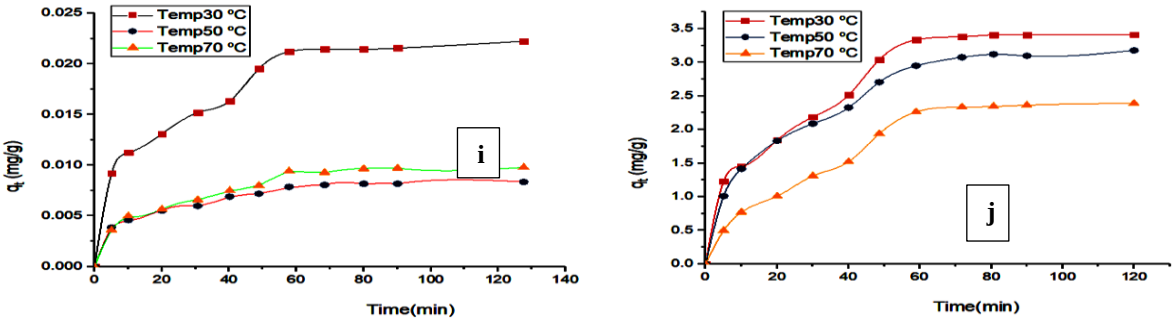

Fig. (7): Effect of different parameters of (a,b) pH solution, (c,d) initial dye concentration, (e,f) adsorbents dose (g,h) particle size (i,j) temperature on adsorption capacity of CAB and HES respectively.

3.8. Adsorption isotherms

The equilibrium adsorption models are necessary for describing the interaction behaviour between solutes and adsorbents and is vital within the scheme of an adsorption system. Equilibrium data, also known as adsorption isotherms, are essential for the design of adsorption systems. These data provide information on the adsorbent's capacity, or the amount needed to remove a unit mass of pollutant under system conditions. Langmuir, and Freundlich's equations were employed to study the adsorption isotherms of the dye**.**

3.8.1. Langmuir assumption isotherm

Langmuir assumption isotherm considers that the monolayer-adsorption take place at the binding's sites with homogenous levels of energy, without interactions among the adsorbed particles and there is no migration of adsorbed particles on the surface of adsorption. The expression of the isotherm model of Langmuir is stated by [32]. The linear plot of C_e/q_e versus C_e as Figure (8) at different initial dye concentration and at different adsorbent dose, it shows that adsorption obeys the Langmuir model and the constants q_m and K_L can be evaluated from the intercept and the slope respectively. Where C_o (mg L^{-1}) is the initial concentration of dye, C_e (mg. L^{-1}) is the organic dye concentration at equilibrium, q_e and q_m (mg. g^{-1}) are the dye amount that adsorbed at equilibrium and the maximum monolayer adsorption capacity, K_L (L.mg^{-1}) is the constant of Langmuir related to the heat of adsorption. The essential characteristic of the Langmuir isotherm could be described by a dimensionless constant R_L referred to as equilibrium parameter calculated by using the data. The R_L value shows the adsorption nature which is Favorable adsorption if $0 < R_L < 1$, Unfavorable adsorption if $R_L > 1$, Linear adsorption if $R_L = 1$ and there will be an Irreversible adsorption if $R_L = 0$ [29].

3.8.2. Freundlich isotherm

The isotherm model of Freundlich is a mathematical expression depended on the multilayer adsorption process on a heterogeneous surface with interaction among the adsorbed molecules. The model is expressed in [29,32]. K_F is an adsorption capacity constant, and n is an empirical parameter indicates the favourability of adsorption process. The n value should be higher than unity for favourable adsorption conditions. The Freundlich constants K_F and n were determined from the linear plot of ln q_e vs ln C_e as displayed in Figure (9) at different initial dye concentration and at different adsorbent dose. The linear correlation coefficients (R^2) i.e., regression factor for Freundlich and Langmuir models are represented in Tables (1, 2). These coefficients are having values always greater than 0.931 except for Langmuir model which includes a value of 0.983. The Langmuir isotherm model has a coefficient of correlation of 0.983 that go with the experimental data than the Freundlich isotherm.

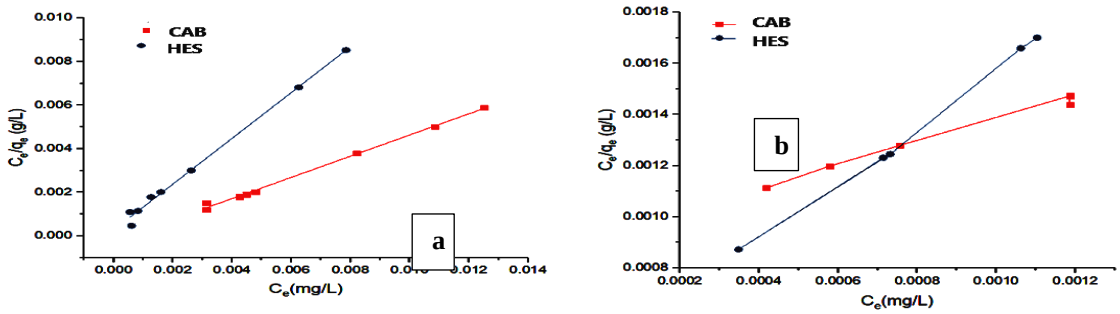

Fig. 8: Langmuir adsorption isotherm plot for the removal of AV19 **(a)** at different initial AV19 concentration and **(b)** at (CAB and HES) dose values of particle size (2.36 mm and 0.355 mm), pH (4 and 2), respectively at 30 °C and 60 min.

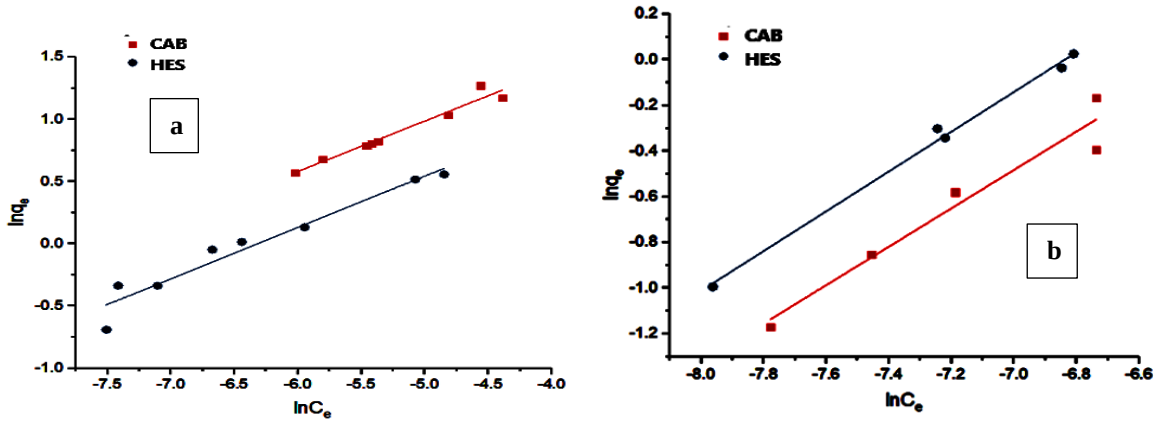

Fig. (9): Freundlich adsorption isotherm plot for the removal of AV19 **(a)** at different initial AV19 concentration and **(b)** at (CAB and HES) dose values of particle size (2.36 mm and 0.355 mm), pH (4 and 2), respectively at 30 °C and 60 min.

Table (1): Comparison of isotherm parameters obtained for the removal of AV 19 on CAB.

Parameters	Langmuir Parameters				Freundlich Parameters		
	q_{max} (mg/g)	K_L x10 (L/mg)	R_L	R^2	K_F (L/mg)	n	R^2
pH	2.058	0.465	0.360	0.996	2.908	2.460	0.953
Initial conc. 3.82 (mg/L)	3.263	0.003	0.988	0.997	3.405	3.067	0.947
Size (mm)	0.992	0.001	0.996	0.986	9.160	3.951	0.991
Dose (g)	2.289	2.152	0.109	0.988	2.893	1.189	0.931
Temperature, °C	5.456	3.889	0.063	0.983	1.184	6.885	0.999

Table (2): Comparison of isotherm parameters obtained for the removal of AV19 on HES.

Parameters	Langmuir Parameters				Freundlich Parameters		
	q_{max} (mg/g)	K_Lx10 (L/mg)	R_L	R^2	K_F (L/g)	n	R^2
pH	0.952	0.266	0.496	0.994	1.988	2.424	0.936
Initial conc. 3.82 (mg/L)	0.002	0.556	0.320	0.997	1.562	2.266	0.948
Size (mm)	2.769	0.001	0.998	0.983	9.490	2.993	0.994
Dose (g)	0.896	0.410	0.399	0.993	3.017	1.148	0.992
Temperature, °C	1.867	2.707	0.088	0.988	1.703	1.103	0.985

3.9. Adsorption Kinetics Studies

The kinetic factors that needed to explain the rate of the process of adsorption, give us valuable information about its modelling and designing. Several kinetic models are applied for the studying of the adsorption process kinetics as pseudo of the first, second order kinetic and intra-particle model of diffusion were applied for the experimental data with different pH, different initial dye concentrations, different doses, various particle sizes and different temperatures for AV19.The adsorption kinetic models as Pseudo-first-order kinetic model, Pseudo-second-order kinetic model and Intra-particle diffusion model were studied. qe ($mg.g^{-1}$) is equilibrium dose of AV19 that adsorbed; qt ($mg.g^{-1}$) is the AV19 dose that adsorbed at time t; k_1 (min^{-1}), k_2 ($g.(mg.\ min)^{-1}$) and k_{int} ($mg.(g.min^{0.5})^{-1}$) are the rate constants of the pseudo first-order, pseudo-second-order and intra-particle diffusion models, respectively; t (min) is the contact time, The kinetic curves of AV19 adsorption onto CAB and HES are presented in Figure (10) and the parameters are shown in Table (3 and 4) for CAB and HES respectively. The correlation coefficients R^2 are also confirmed that the process of adsorption was better fitted by the pseudo-second order of the kinetic model, indicating that intra-particle diffusion was not the only rate-limiting step [34], as consistent with the results of the fits to the pseudo-second-order kinetic and intra-particle diffusion models. suggesting that the adsorption process is indicative of a chemisorption mechanism [35-37]. Error analysis was carried out by estimating normalized standard deviations (NSD) and calculated by equation reported in [29]. As reported in previous theories, the pseudo of the second order model is dependent upon the theory that the rate of the determining step could also be a chemical sorption including valence forces through the spreading the electrons among the adsorbate and adsorbent. [38-40].

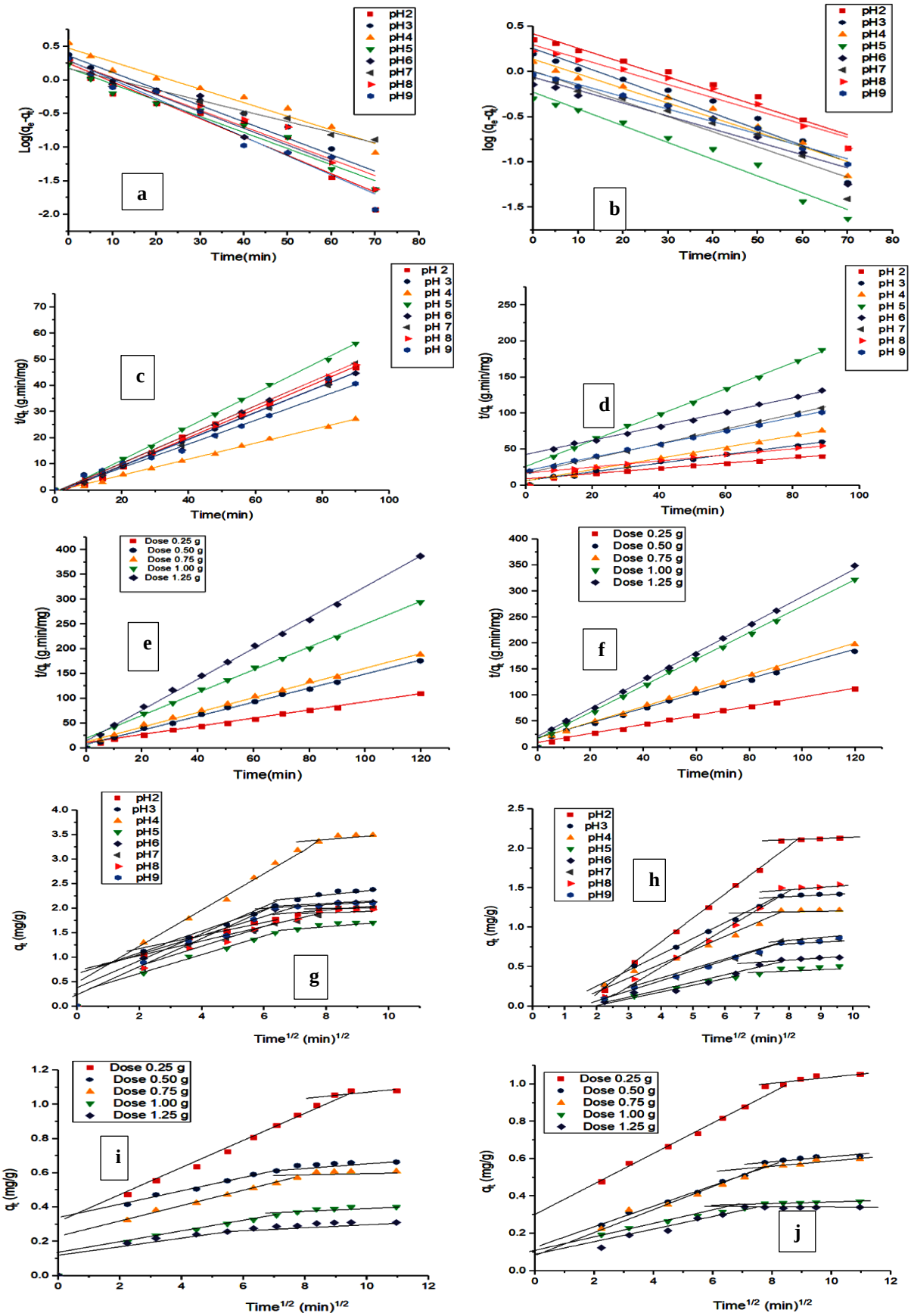

Fig. (10): (a,b) Pseudo-First-order Kinetic, (c-f) Pseudo-Second-order Kinetic and (g-j) Intraparticle Diffusion Kinetic model for the removal of AV19 at different pH solution and adsorbents dose of CAB and HES at particle (2.36 and 0.355 mm) with initial AV19 concentration 3.82 mg/L, 30 °C and 60 min.

Table (3): Kinetic parameters for the adsorption of AV19 on CAB:

Parameters	Pseudo first order model			Pseudo second order model				Intra particle diffusion model	
	q_{e1} (mg/g)	K_1 (min^{-1})	R^2	q_{e2} (mg/g)	K_2 (g /mg min)	R^2	NSD	K_{in} (g/mg min^{-1})	R^2
pH2	1.889	0.063	0.930	1.837	0.18،	0.990	0.615	0.190	0.858
pH3	2.288	0.057	0.945	2.198	0.379	0.990	0.580	0.234	0.916
pH4	2.972	0.047	0.963	3.261	0.223	0.990	0.470	0.370	0.959
pH5	1.510	0.055	0.963	1.568	0.327	0.990	0.760	0.175	0.928
pH6	1.911	0.058	0.943	1.960	0.319	0.990	0.829	0.214	0.907
pH7	1.483	0.119	0.966	1.825	0.519	0.980	0.680	0.203	0.943
pH8	1.907	0.056	0.947	1.817	0.379	0.990	0.601	0.202	0.931
pH9	1.950	0.065	0.951	1.951	0.224	0.990	0.832	0.214	0.891
Initial conc. mg/L 3.82	3.939	0.041	0.941	6.137	0.022	0.990	1.531	0.378	0.873
7.64	4.253	0.038	0.946	6.036	0.015	0.980	1.045	0.491	0.915
11.46	3.782	0.036	0.961	5.469	0.016	0.980	1.543	0.492	0.947
15.28	4.458	0.040	0.955	6.217	0.015	0.980	1.032	0.495	0.911
26.74	3.743	0.029	0.948	5.302	0.008	0.980	1.250	0.500	0.947
Dose, g 0.25	0.852	0.034	0.955	1.213	0.062	0.990	0.989	0.094	0.931
0.50	0.404	0.040	0.938	0.705	0.271	0.990	0.435	0.050	0.743
0.75	0.485	0.044	0.912	0.673	0.179	0.990	0.644	0.050	0.843
1.00	0.322	0.044	0.943	0.434	0.269	0.990	0.764	0.034	0.875
1.25	0.198	0.046	0.930	0.321	0.677	0.990	0.766	0.024	0.756
Size, mm 3.20	1.304	0.651	0.909	1.740	0.099	0.994	0.843	0.088	0.917
2.36	1.750	0.064	0.914	2.240	0.104	0.997	0.551	0.102	0.885
0.850	1.743	0.066	0.931	1.610	0.104	0.996	0.643	0.101	0.891
Temperature, ˚C 30	2.028	0.041	0.939	2.280	0.050	0.990	0.542	0.118	0.929
50	1.542	0.045	0.933	3.181	0.063	0.990	0.464	0.154	0.915
70	2.011	0.041	0.955	3.240	0.050	0.990	0.421	0.161	0.938

3.10. Adsorption Thermodynamic

Knowing the parameters of thermodynamic offer a great information of the inherent energetic that related to adsorption. Gibbs free energy changes (ΔG°), entropy (ΔS°), and enthalpy (ΔH°) were calculated using data from Figure (11), where $K_d = q_e/C_e$ is the distribution coefficient. $\Delta H°$ and $\Delta S°$ values were calculated by drawing a plot of ln K_d *vs* 1/T, where T is the temperature in (*K*), and taking the slope and intercept from Figure (11). for CAB and HES then the value of $\Delta G°$ was calculated using the equation presented in [37]. The results are shown in Table (5) show a spontaneous and favourable adsorption process over the entire temperature range ($\Delta G^\circ < 0$) in adsorption of AV19 on CAB, the positive value of ΔH° obtained indicated that the dye adsorption process is an endothermic [41]. The positive value of ΔS° proposes an increase within the randomness at the solid/solution interface take place at the inner structure of the adsorption of dyes onto adsorbents [40- 43]. The value of ΔG° found during this work suggested that the AV19 adsorption on CAB was a chemisorption process. on other hand $\Delta G^\circ > 0$ for AV19 adsorption on HES suggested that the adsorption was physisorption, the negative value of ΔH° obtained showed that the dye adsorption process in an exothermic. The negative ΔS° value suggests the formation of order activated complex and associated mechanism for the adsorption this results agreement with [42-45].

Table (4): Kinetic parameters for the adsorption of AV19 on HES:

Parameters	Pseudo first order model			Pseudo second order model				Intra particle diffusion model	
	q_{e1} (mg/g)	K_1 (min^{-1})	R^2	q_{e2} (mg/g)	K_2 (g /mg min)	R^2	NSD	K_{in} (g/mg min^{-1})	R^2
pH2	2.615	0.036	0.952	2.750	0.015	0.998	0.501	0.282	0.964
pH3	1.803	0.041	0.930	1.660	0.056	0.999	0.763	0.166	0.951
pH4	1.370	0.037	0.956	1.283	0.099	0.998	0.902	0.141	0.961
pH5	0.591	0.042	0.962	0.556	0.123	0.099	0.965	0.063	0.970
pH6	0.867	0.033	0.918	1.018	0.022	0.997	0.643	0.086	0.953
pH7	1.015	0.038	0.920	0.974	0.063	0.999	0.704	0.107	0.967
pH8	1.973	0.033	0.955	2.377	0.011	0.998	0.562	0.210	0.968
pH9	0.991	0.031	0.984	1.083	0.042	0.999	0.601	0.108	0.975
Initial Conc. mg/L 3.82	0.333	0.039	0.951	1.210	0.062	0.996	0.521	0.027	0.918
7.64	0.530	0.036	0.950	0.705	0.271	0.996	0.535	0.039	0.892
11.46	0.389	0.041	0.946	0.673	0.179	0.983	0.611	0.041	0.899
15.28	0.332	0.052	0.930	0.434	0.269	0.998	0.734	0.045	0.909
26.74	0.473	0.062	0.977	0.321	0.677	0.996	0.852	0.058	0.898
Dose, g 0.25	0.169	0.034	0.955	1.148	0.082	0.999	0.753	0.073	0.951
0.50	0.544	0.040	0.938	0.705	0.109	0.998	0.423	0.047	0.941
0.75	0.524	0.043	0.912	0.655	0.134	0.986	0.553	0.045	0.936
1.00	0.312	0.044	0.943	0.392	0.398	0.993	0.589	0.027	0.913
1.25	0.355	0.045	0.932	0.372	0.341	0.989	0.601	0.025	0.803
Size, mm 0.850	3.274	0.045	0.954	3.557	0.012	0.996	0.403	0.234	0.906
0.355	3.300	0.046	0.954	4.337	0.029	0.999	0.400	0.250	0.932
0.180	3.058	0.063	0.879	3.389	0.024	0.993	0.451	0.187	0.914
Temperature, ˚C 30	3.250	0.044	0.922	3.747	0.019	0.999	0.542	0.272	0.921
50	2.824	0.039	0.966	3.463	0.022	0.995	0.632	0.268	0.945
70	2.212	0.028	0.992	2.868	0.013	0.999	0.821	0.251	0.918

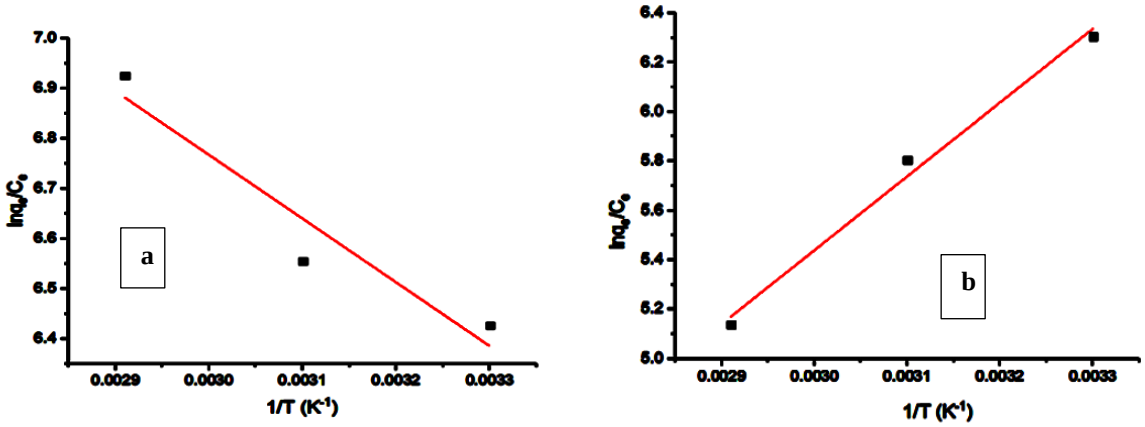

Fig. 11(a): The Thermodynamic parameters for the removal of AV19 at different range of temperature with initial AV19 concentration 3.82 mg/L by adsorbent dose 0.75 g for **(a)** CAB and **(b)** HES of particle size (2.36 and 0.355 mm) pH (4 and 2) and 60 min.

Table (5): Thermodynamic Parameters of AV19 adsorbed on CAB and HES.

Temperature, °C		Thermodynamic Parameters		
		ΔG° (KJ/mol)	ΔH° (KJ/mol)	ΔS° (KJ/mol)
CAB	30	-1.938	1.274	0.011
	50	-2.149		
	70	-2.362		
HES	30	26.466	-3.531	0.099
	50	28.446		
	70	30.426		

4.Conclusions

The ability of CAB and HES as a bio-waste adsorbent to remove AV19 from solutions was examined. Some parameters as pH values, initial dye concentrations, adsorbent doses, adsorbent sizes, and temperatures were found to affect the adsorption efficiency of CAB and HES. The kinetic data show that the operation of adsorption follows the pseudo of second order kinetic, indicating chemisorption's. The adsorption data present the best fit to the Langmuir model, suggesting that adsorption occurs by the formation of a monolayer. The thermodynamic parameter show that adsorption is spontaneous and endothermic in nature in case of CAB and exothermic for HES. This study proved that CAB and HES could be used as unique and cheap adsorbents for dye removal treatment and are also used as a good low-cost naturally adsorbent material for many anionic and cationic dyes.

Acknowledgements:

The authors acknowledge Prof. Dr. Omaima Hussein (Department of Chemistry, College of Science, Taif University, Saudi Arabia) for English revision.

Declarations

Conflicts of interest: There are no conflicts to declare.

Formatting of funding sources

No funding sources

References

1. Ummalyma, S. B., Sahoo, D. and Pandey, A.: Resource recovery through bioremediation of wastewaters and waste carbon by microalgae: a circular bioeconomy approach. J. Enviro. Sci. and Poll. Rese., 28, 58837-58856 (2021).
2. Kumar, L., Chugh, M., Kumar, S., Kumar, K., Sharma, J. and Bharadvaja, N.:Remediation of petrorefinery wastewater contaminants: A review on physicochemical and bioremediation strategies. J. Proc. Safety and Enviro. Protec., 83, 821-832 (2022).
3. Ejikeme, E. M., Ejikeme, A. and Benjamin, N.: Equilibrium, Kinetics and Thermodynamic Studies on MB Adsorption Using Hamburger Seed Shell Activated Carbone. J. Eng. Techno. 14, 74-83(2014).
4. Sun, M.M., Ye, M., Schwab, A.P., Li, X., Wan, J.Z., Wei, Z., Wu, J., Friman, V.P., Liu, K., Tian, D., Liu, M.Q., Li, H.X., Hu, F. and Jiang, X.: Human migration activities drive the fluctuation of ARGs: case study of landfills in Nanjing, eastern China of landfills in Nanjing, eastern China. J. Hazard. Mater., 315, 93-101 (2016).
5. Arun, K., Panmei, G. and Uzma, N.: Adsorption Equilibrium and Kinetics of Crystal Violet Dye from Aqueous Media onto Waste Material. J.Chem. Sci. Rev. and Letters, 3, 1-13(2014).
6. Karimifard, S. and Moghaddam, A. R. M.: Application of response surface methodology in physicochemical removal of dyes from wastewater: A critical review. Science of the Total Environment., 640, 772-797. (2018).
7. Deniz, F.: Dye removal by almond shell residues: studies on biosorption performance and process design. J. Mater. Sci. Eng., 33, 2821-2826 (2013).
8. El Haddad, M., Mamouni, R., Saffaj, N. and Lazar, S.: Removal of a cationic dye – Basic Red 12 – from aqueous solution by adsorption onto animal bone meal. J. Association of Arab Universities for Basic and Applied Sciences., 12, 48-54(2021).
9. Sutar, S., Patil, P. and Jadhav, J.: Recent advances in biochar technology for textile dyes wastewater remediation: A review. J. Enviro. Rese., 11, 28-41 (2022).
10. Nidheesh, N.P., Zhou, M. and Oturan, M. A.: An overview on the removal of synthetic dyes from water by electrochemical advanced oxidation processes. J. Chemosphere., 197, 210-227 (2018).
11. Abbas, R., Hosseinali, R., Ahmad, J. and Ali, K.: Surface modification of bone char for removal of formaldehyde from air. J. Appl. Surf. Sci., 286, 235-239 (2013).
12. Pirvutoiu, I. and Popescu, A.: Research on the major trends in the romanian egg market. Bull. Univ. J. Agric. Sci. Vet., 69, 229-238 (2021).
13. Anastopoulos, I., Ahmed, M. J. and Hummadi, E. H.: Eucalyptus-based materials as adsorbents of heavy metals and dyes pollutants from (waste) waters. J. Mole. Liqui., 11, 64-88 (2022).
14. Elkady, M.F., Amal, M., Ibrahim, M. and Abd El-Latif, M.: Assessment of the adsorption kinetics, equilibrium and thermodynamic for the potential

removal of reactive red dye using eggshell biocomposite beads. J. Desalination., 278, 412-423 (2011).

15. El Haddad, M., Mamouni, R., Saffaj, N. and Lazar, S.: Removal of two textile dyes from aqueous solutions onto calcined bones. J. Assoc. Arab Univ. Bas & Appli. Sci., 14, 51-59 (2013).

16. Mkukuma, L.D., Skakle, J.M.S., Gibson, I.R., Imrie, C.T., Aspden, R. M. and Hukins, D.W.L.: Effect of the proportion of organic material in bone on thermal decomposition of bone mineral., J. Calcified Tissue Inter.,75, 321-328(2004).

17. Paschalis, E.P., Betts, F., DiCarlo, E., Mendelsohn, R. and Boskey, A.L.: FTIR microspectroscopic analysis of normal human cortical and trabecular bone. J. Calcified Tissue Inter., 61, 480-486 (1997).

18. Murugan, R., Ramakrishna, S. and Rao, K.P.: Nanoporous hydroxy-carbonate apatite scaffold made of natural bone. J. Mater. Lett. 60, 2844-2847 (2006).

19. Figueiredo, M., Fernando, A., Martins, G., Freitas, J., Judas, F. and Figueiredo, H.: Effect of the calcination temperature on the composition and microstructure of hydroxyapatite derived from human and animal bone. J. Ceramics Inter., 36, 2383-2393 (2010).

20. Guru, P.S. and Dash, S.: Amino acid modified eggshell powder (AA–ESP) – a novel bio-solid scaffold for adsorption of some styryl pyridinium dyes. J. Dispersion Sci. Technol., 34, 1099-1112 (2013).

21. Arshadi, M., Faraji, A.R., Amiri, M.J., Mehravar, M. and Gil, A.: Removal of methyl orange on modified ostrich bone waste – A novel organic–inorganic biocomposite. J. Coll. Inter. Sci., 446 11-23 (2015).

22. Panneerselvam, P., Morad, N. and Tan, K.: Magnetic nanoparticle (Fe_3O_4) impregnated onto tea waste for the removal of nikel (II) from aqueous solution. J. Hazard Mater., 196, 160-167 (2011).

23. Partha, S. and Sukalyan, D.: Sorption on eggshell waste—A review on ultrastructure, biomineralization and other applications. J. Advances in Colloid and Interface Science., 209, 49-67 (2014).

24. Agarwal, B., Balomajumder, C. and Thakur, P.K.: Simultaneous co-adsorptive removal of phenol and cyanide from binary solution using granular activated carbon. J. Chem. Eng., 228, 655-664 (2013).

25. Stavropoulos, G.G., Skodras, G.S., Papadimitriou, K.G.: Effect of solution chemistry on cyanide adsorption in activated carbon. J. Appl. Therm. Eng,.74, 182-185 (2015).

26. Noureddine, B., Hassiba, M., Zahra, S. and Mohamed, T.: Biosorption of cationic dye from aqueous solutions onto lignocellulosic biomass (Luffa Cylindrica): characterization, equilibrium, kinetic and thermodynamic studies. Int. J. Ind Chem., 1-14 (2016).

27. Hojjati- Najafabadi, A., Mansoorianfar, M., Liang, T., Shahin, K. and Karimi-Maleh, H.: A review on magnetic sensors for monitoring of hazardous pollutants in water resources. J. Sci. Enviro., 824, 153-844 (2022).

28. Mohammadine, E.: Removal of Basic Fuchsin dye from water using mussel shell biomass waste as an adsorbent: Equilibrium, kinetics, and thermodynamics. J. Taibah Univ. Sci., 10, 664-674 (2016).

29. Heba, M. E., Asrar, G., Nagwa, B., Fatema, A. G. and Samia, A. Agricultural by-products as green chemistry in elimination of RR43 from aqueous media- adsorption properties and thermodynamic study. J. Egyptian Chemistry, 65,1-12(2022).

30. Davoud, B., Edris, B. and Ferdos, K. M.: Equilibrium, Kinetic Studies on the Adsorption of Acid Green 3 (Ag3) Dye onto Azolla filiculoides as Adsorbent. J.Am. Chem.Sci., 11, 1-10 (2016).

31. Emmanuel, O.O. and Felix, A.T.: Removal of methylene- blue from aqueous solution using alkali-modified malted sorghum mash.J. Eng. Environ. Sci., 36, 161-169 (2021).

32. Abeer, A.E., Mohamed, A.A.: Removal of some advanced dyes from aqueous solution using modified kaolinite clay. Al-Azhar Bulletin of Science., 31: 59-68 (2020).

33. Amir, H.M., Mehdi, V., Mohammad, J. M., Anvar, A., Bayram, H., Amir, Z. and Soudabeh, P.: Sodium Dodecyl Sulfate Modified-Zeolite as a promising Adsorbent for the Removal of Natural Organic Matter from Aqueous Environments. J. health Scope., 5, 1-8 (2016).

34. Thai, A.N., Vinh, T.N., Thi, T., Hieu, T., and Nhat, H.N.: Batch and column adsorption of reactive dyes by eggshell powder–chitosan gel core-shell material. Mor. J. Chem. 9: 18-27 (2021).

35. Iwuozor, K. O., Emenike, E. C., Aniagor, C. O., Iwuchukwu, F. U., Ibitogbe, E. M., Temitayo, O. B. and Adeniyi, A. G.: Removal of pollutants from aqueous media using cow dung-based

adsorbents. J. Current Rese. in Green and Sustainable Chem., 100300 (2022).

36. Wang, L. and Li, J.: Adsorption of C.I. Reactive red 228 dye from aqueous solution by modified cellulose from flax shive: kinetic, equilibrium and thermodynamics. J. Ind. Crops and Prod., 42, 153-158 (2013).

37. Yang, S., Li, L., Pei, Z., Li, c., Lv, J., Xie, J., Wen, B. and Zhang, S.: Adsorption kinetic, isotherms and thermodynamics of Cr (III) on graphene oxide. J. Colloids and Surface A: Physic. chem. Eng. Aspects., 457, 100-106 (2014).

38. Raji, F. and Pakizeh, M.: Kinetic and thermodynamic studies of Hg (II) adsorption onto MCM-41 modified by ZnCl2. J. Appl. Sur. Sci., 301, 568-575 (2014).

39. Manimekalai, T. K., Sivakumar, N. and Periyasamy, S.: Real-world mixed plastics waste into activated carbon and its performance in adsorption of basic dyes from textile effluent. Digest. J. Nanomater. Biostru., 10, 985-1001 (2015).

40. Maher, E.S., Ahmed, A.E. and Amal, H.M.: Effectiveness of Sunflower Seed Husk Biochar for Removing Copper Ions from Wastewater. a Comparative Study. J. Soil and Water Res., 11, 53-63 (2016).

41. El maguana, Y., Elhadiri, N., Benchanaa, M. and Chikri, R.: Adsorption Thermodynamic and Kinetic Studies of Methyl Orange onto Sugar Scum Powder as a Low-Cost Inorganic Adsorbent., J. Hinda. Chem.2020, 1-10 (2020).

42. Lakkaboyana, S. K., Soontarapa, K., Marella, R. K., and Kannan, K.: Preparation of novel chitosan polymeric nanocomposite as an efficient material for the removal of Acid Blue 25 from aqueous environment. International Journal of Biological Macromolecules, 168, 760-768 (2021).

43. Fatema, A., Heba, M. E., Asrar, G., Nagwa, B., Samia, E. A. and Abeer, E.: Bio-waste as eco-friendly adsorbent for the removal of hazardous dyes. J. Al-Azhar Bulletin of Sci., 33, 1-12 (2022).

44. Jazi, M.B., Arshadi, M., Amiri, M. J and Gil, A.: Kinetic and thermodynamic investigations of Pb (II) Cd (II) adsorption on nanoscale organo-functionalized SiO2-Al2O3. J. Coll. Inter. Sci., 422, 16-24 (2014).

45. El-Bindary, M. A., El-Desouky, M. G., and El-Bindary, A. A.: Adsorption of industrial dye from aqueous solutions onto thermally treated green adsorbent: A complete batch system evaluation. J. Mole. Liqui, 30, 117-182 (2021).